appropriate thickness for measuring the reflection intensity in the Laue case, we can expect a large change in the ratio of intensity across the absorption edge as a function of the temperature factor.

Since this temperature effect is quite conspicuous, we can point out some possible applications on making use of it. For example, we can determine the temperature factor $B$ from experiment if we know the values of normal- and anomalous-scattering factors. The calculated atomic scattering factors are reliable and agree with experimental values within an error of 1%. The anomalous-scattering factors are not so reliable. Near the absorption edge, the anomalous-scattering factors depend on the surroundings of the absorbing atoms and have some fine structures corresponding to XANES (X-ray absorption near edge structure) and EXAFS (extended X-ray absorption fine structure). The values for an isolated atom calculated by the formula of Parratt & Hempstead (1954) are sometimes different from the actual values in condensed matter. However, in the energy range of more than 100 eV from the absorption edge, XANES or EXAFS does not affect very much the values of the anomalous-scattering factor. The values calculated for isolated atoms in most cases agree with experimental ones within an error of 10%. Then, if we have precise values of the anomalous-scattering factors $f'$ and $f''$, we can determine the temperature factor $B$ by use of the temperature effect. The advantage of this approach is that we need only one reflection for determination of the temperature factor. The temperature factor determined in the present experiment is $B = 0{\cdot}20$ Å$^2$ at liquid-nitrogen temperature and $B = 0{\cdot}63$ Å$^2$ at room temperature, by assuming the anomalous-scattering factors obtained for an isolated Ge atom.

The authors would like to thank Mr H. Sugawara for his assistance in the experiment. This work was partly supported by a Grant-in-Aid for Scientific Research (57420012).

### References

BATTERMAN, B. W. & CHIPMAN, D. R. (1962). *Phys. Rev.* **127**, 690-693.
CROMER, D. T. (1965). *Acta Cryst.* **18**, 1[illegible]23.
CROMER, D. T. & MANN, J. B. (1968[illegible] *Acta Cryst.* **A24**, 321-324.
DATSENKO, L. I., SKOROKHOD, M. YA. & VASILKOVSKI, A. S. (1968). *Phys. Status Solidi*, **30**, 231-237.
FUKAMACHI, T., HOSOYA, S. & OKUNUKI, M. (1976). *Acta Cryst.* **A32**, 104-109.
FUKAMACHI, T., KAWAMURA, T., HAYAKAWA, K., NAKANO, Y. & KOH, F. (1982). *Acta Cryst.* **A38**, 810-813.
KAWAMURA, T. & FUKAMACHI, T. (1979). *Acta Cryst.* **A35**, 831-835.
LUDEWIG, J. (1969). *Acta Cryst.* **A25**, 116-118.
PARRATT, L. G. & HEMPSTEAD, C. F. (1954). *Phys. Rev.* **94**, 1593-1600.

*Acta Cryst.* (1986). A**42**, 116-122

# Asymptotic Bragg Diffraction. Single-Crystal Surface-Adjoining-Layer Structure Analysis

BY A. M. AFANAS'EV, P. A. ALEKSANDROV, S. S. FANCHENKO, V. A. CHAPLANOV AND S. S. YAKIMOV

*I. V. Kurchatov Institute of Atomic Energy*, 123182 *Moscow, USSR*

(*Received* 28 *June* 1985; *accepted* 11 *October* 1985)

### Abstract

The angular dependence of the X-ray pure-diffraction intensity $I(\theta)$ has been measured in Ge and Si single crystals (surface covered with natural oxide films) by means of triple-crystal diffractometry. Measurements were extended to specimen-crystal angular deviations from the Bragg angle of up to 500 Bragg-peak half-widths. The $I(\theta)$ data at such large deviation angles are informative of both static and dynamic Debye-Waller-factor variation over crystal depth, the achievable spatial resolution turning out to be of the order of 1 nm. The high spatial resolution of the asymptotic Bragg diffraction made it necessary to consider in theory the layer-to-layer variation of both the scattering characteristics (Debye-Waller factor) and the interplanar spacings. A theoretical treatment of the problem is presented. Reconstructed Debye-Waller factors for the first four atomic planes, counting from the crystal-oxide boundary, are 0·3, 0·4, 0·7, 0·7 and 0·6, 0·6, 0·9, 1 for Ge and Si, respectively.

## 1. Introduction

X-ray diffraction methods play an important role in crystal-surface research. Triple-crystal diffractometry (TCD) is based upon a highly accurate analysis of the specimen-scattered X-ray angular distribution (the latter being measured by means of the third, *i.e.* analyzer, crystal). The TCD makes it possible to separate the purely diffractive scattering from the accompanying diffuse scattering on crystal-lattice defects

0108-7673/86/020116-07$01.50 

(Eisenberger, Alexandropoulos & Platzman, 1972; Iida, 1979; Iida & Kohra, 1979; Afanas'ev, Koval'chuk, Lobanovich, Imamov, Aleksandrov & Melkonyan, 1981). Moreover, a very limited analyzer-crystal 'acceptance window' (usually comprising several arc s) drastically reduces the background. As a result, one is able to measure the diffraction intensity at very large specimen-crystal angular deviations $\Delta\theta$ from the Bragg angle, namely, three orders of magnitude above the Bragg-peak half-width. Besides determining the diffraction peak amplitude one can establish its shape $i(\Delta\theta_3)$, where $\Delta\theta_3$ is the analyzer-crystal rotation angle. In the case of purely diffractive scattering, the angular distribution law $i(\Delta\theta_3)$ should remain invariable. These circumstances enable one to make reliable measurements of pure diffraction at very large crystal deviation angles $\Delta\theta$ when $I(\Delta\theta)$ is several million times below its value $I(0)$, *i.e.* at exactly the Bragg-law angle.

Diffraction measurements performed deliberately very far away from the Bragg-law angle (asymptotic Bragg diffraction) provide valuable information on crystal perfection in thin surface-adjoining layers and near the boundary surfaces (Afanas'ev, Aleksandrov, Imamov, Lomov, Zavyalova, 1984; Yakimov, Chaplanov, Afanas'ev, Aleksandrov, Imamov & Lomov, 1984). The most significant physical feature of the diffraction scattering process under these conditions is, indeed, the fact that, despite the high X-ray penetration power, the large-angle diffraction scattering phenomena mainly take place in a surface- or boundary-adjoining layer, the thickness of which becomes less the further one goes from the Bragg angle. Indeed, the diffraction partial waves originating from perfect-crystal inner atomic layers do cancel each other one by one. Hence, X-ray diffractometry opens quite unique opportunities of testing the degree of structure perfection of the thinnest surface-adjoining crystal layers down to single monoatomic layers. The application of this method to investigate superfinish-surface Ge crystals was reported by Yakimov, Chaplanov, Afanas'ev, Aleksandrov, Imamov & Lomov (1984). As the measurements were carried out under normal conditions and not in vacuum, an oxide film appeared on the crystal surface. The analysis of the experimental data made it possible to estimate the thickness of the crystal–oxide boundary transition layer as approximately 1 nm. In this transition zone, consisting of only 4–5 monoatomic layers, the static Debye–Waller factor was found to be sharply reduced. The present paper reports results of similar measurements for Si monocrystals, simple estimates suggesting the presence of a transition layer comprising no more than three monolayers. As a result, there arose both the need and, on the other hand, a real possibility to determine the degree of order–disorder for each individual monoatomic layer inside the transition sheath.

In § 2 we treat the theoretical basis of the method. § 3 describes the corresponding experimental techniques, presents the experimental data and the results of data analysis. The analysis involves both the present Si crystal experimental data and the Ge crystal experimental results, reported by Yakimov, Chaplanov, Afanas'ev, Aleksandrov, Imamov & Lomov (1984). The prospects and limitations of the present method are discussed in § 3.

## 2. Theory

The diffraction reflection of X-rays at incidence angles $\theta$ such that the $\Delta\theta = \theta - \theta_B$ difference sufficiently exceeds the Darwin 'table' width $\theta_0$ ($\theta_B$ representing the Bragg angle) is described with simple kinematic theory, based upon the common perturbation theory. In the symmetric reflection case (Fig. 1) the reflection coefficient $R$ can be expressed in terms of total crystal X-ray scattering amplitude $M$ in the following way:

$$R = (4\sin^2\theta)^{-1}|M|^2.$$

The total X-ray scattering amplitude $M$ for a semi-infinite crystal is the sum of partial scattering amplitudes $M_n(\theta)$, representing X-ray scattering either from individual reflecting atomic planes or from close-lying plane pairs [as in the case of (111) reflection from diamond-like lattice crystals]:

$$M(\theta) = \chi_h(\theta)(\pi/\sin\theta_B)\sum_{n=1}^{\infty} M_n(\theta) \qquad (1)$$

$$M_n(\theta) = \exp[-W_n(\theta) + 2\pi i(\cot\theta_B\,\Delta\theta\, n + u_n/a_0)]$$

with $\chi_h(\theta)$, $\exp[-W_n(\theta)]$, $u_n$ and $a_0$ representing the $h$ Fourier component of the elementary cell polarizability, the $n$th atomic plane Debye–Waller factor, the $n$th atomic plane displacement from its ideal crystal position and the spacing between reflecting planes, respectively.

Accordingly, in the case of symmetric X-ray reflection from a crystal, the reflection coefficient is expressed as follows:

$$R = \left|[\pi\chi_h(\theta)/2\sin\theta\sin\theta_B]\sum_{n=1}^{\infty} M_n(\theta)\right|^2. \qquad (2)$$

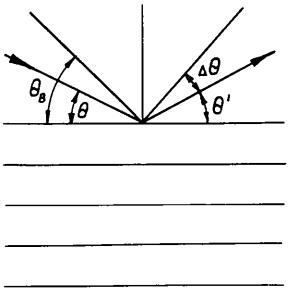


Fig. 1. X-ray reflection from crystal scheme ($\theta$ incidence angle, $\theta' = \theta$ – reflection angle, $\theta_B$ Bragg angle, $\Delta\theta = \theta - \theta_B$).

The angular dependence of $\chi_h(\theta)$ is found from the expression

$$\chi_h(\theta)=\chi_h F(\sin\theta\lambda^{-1})S(\theta)/F(\sin\theta_B\lambda^{-1})S(\theta_B)$$

with $F(\sin\theta/\lambda)$, $\lambda$ and $S(\theta)$ representing the form factor, the X-ray wavelength and a geometric structural factor, introduced for considering diffraction from crystals with more than one atom per unit cell, respectively.

When treating diffraction problems which involve only small deviations of the incidence angle $\theta$ from the Bragg angle, it is common practice to neglect any angular dependence on the part of both the phase volume $[4\sin^2\theta]^{-1}$ and the polarizability square $|\chi_h(\theta)|^2$, substituting in the reflection coefficient formula (2) the corresponding constant factors $[4\sin^2\theta_B]^{-1}$ and $|\chi_h(\theta_B)|^2$. However, in the case of asymptotic Bragg diffraction the angular dependences of the phase volume, atomic form factor and structural factor become essential. When they are taken to account, it is convenient to single out the following factor:

$$A(\theta)=\left|\frac{\chi_h S(\theta)F(\sin\theta\lambda^{-1})}{2\sin\theta S(\theta_B)F(\sin\theta_B\lambda^{-1})}\right|^2.$$

In the case of diffraction reflection with $\Delta\theta\sim\theta_0$ the diffracted waves are formed over a large number of atomic planes. Accordingly, the diffraction reflection amplitude can be expressed as an integral instead of the sum in (1). The reflection coefficient is then represented as follows:

$$R(\theta)=A(\theta)K^2\left|\int_0^\infty dz\exp[-W(z)+i\varphi(z)+iqz]\right|^2$$

$$q=2K\cos\theta_B\,\Delta\theta,\qquad K=2\pi/\lambda.$$

Here, the function $\varphi(z)$ describes the atomic plane displacement, while $\exp[-W(z)]$ represents the Debye–Waller-factor variation near the surface. The Debye–Waller factor can be expressed as a product of a dynamic factor, representing the oscillations of atoms around their equilibrium position, and a static factor, resulting from irregular atom displacements from their positions in the ideal crystal.

In the ideal crystal there are no atomic-plane displacements and, consequently, $\varphi(z)=0$. Any dynamic Debye–Waller-factor variations can also be neglected. Then one arrives at the following simple and well known formula

$$I(\theta)=I_0A(\theta)(\Delta\theta)^{-2}$$

with $I_0$ a constant factor.

Consider now the case of sufficiently large $\Delta\theta$ angular differences and of crystals with $W(z)$ and $\varphi(z)$ functions slowly varying in the subsurface (*i.e.* surface-adjoining) region. One can integrate by parts the intensity formula, whereby

$$\int_0^\infty dz\exp[-W(z)+i\varphi(z)+iqz]$$
$$=\exp[-W(0)+i\varphi(0)]/iq$$
$$-\int_0^\infty dz(e^{iqz}/iq)\,d/dz\{\exp[-W(z)+i\varphi z]\}.$$

In the asymptotic case $\Delta\theta\gg\theta_0L_{ex}/L$ (with $L$ and $L_{ex}$ representing the subsurface-layer inhomogeneity scale and extinction depth, respectively), the second term in the above formula becomes negligible. Consequently, the following expression for the intensity is obtained:

$$I(\theta)=I_0[A(\theta)/\Delta\theta^2]\exp[-2W(0)].$$

Thus, in the asymptotic case $\Delta\theta/\theta_0\gg L_{ex}/L$ the intensity of X-ray diffraction does not depend on atomic-plane displacement and is determined by the Debye–Waller-factor value on the surface. This means that at sufficiently large $\Delta\theta$ the diffracted wave formation occurs in the surface-adjoining region. This is so despite the fact that far from the Bragg angle the X-ray penetration depth is determined by the usual absorption mechanism and exceeds substantially the extinction depth, which, in turn, can be considerably greater than the crystal structure disturbance depth. It can readily be seen from the intensity formula that the thickness $L_\theta$ of the layer, active in the formation of the diffracted wave, is related to the deviation $\Delta\theta$ from the Bragg angle in the following simple way: $L_\theta\simeq L_{ex}\theta_0/\Delta\theta$.

Thus, the investigation of diffraction at sufficiently great $\Delta\theta$ permits one to obtain information about very thin sub-surface layers. It was shown by Afanas'ev, Aleksandrov, Imamov, Lomov & Zavyalova (1984) and Yakimov, Chaplanov, Afanas'ev, Aleksandrov, Imamov & Lomov (1984) that the experimentally achieved values of $\Delta\theta$ make it possible to judge transition layers with a thickness corresponding to three to four interplane spacings. In this case the continuous crystal structure model is no longer applicable, and it becomes necessary to consider discrete atomic planes. The following is the first discussion of a discrete-type asymptotic Bragg diffraction analysis.

For the sake of simplicity, let us first restrict our analysis to the case of zero atomic-plane displacement. Assume only the first $N$ atomic layers to be disturbed, each of them having a given Debye–Waller factor defined in the following way:

$$\exp[-W_n(\theta)]=\begin{cases}\exp[-8\pi^2(\langle u_n^2\rangle/\lambda^2)\sin^2\theta] & n\le N\\ 1 & n>N.\end{cases}$$

Here $\langle u_n^2\rangle^{1/2}$ represents the $n$th layer root-mean-square displacement.

Neglecting the insignificant angular dependence of the Debye-Waller factor, *i.e.* substituting $W_n(\theta_B)$ instead of $W_n(\theta)$, one easily obtains the following expression for the diffraction intensity:

$$I(\theta) = I_0[A(\theta)/\Delta\theta^2] \times \left| \sum_{n=1}^{N} X_n \exp[iQ(n-N-1)](1-e^{iQ})+1 \right|^2$$

$$X_n = \exp[-W_n(\theta_B)], \qquad Q = 2\pi \cot\theta_B \, \Delta\theta.$$

In fact, this intensity expression is dependent upon $N$ parameters $X_n$, the latter characterising the degree of structure perfection of each of the atomic planes inside the transition-layer thickness $Na_0$. In the case of small $N$ this formula for the intensity can be directly applied to analyze the diffraction angular dependence experimental data. By means of $X_n$ parameter variations, one can achieve a good agreement of theory and experiment. When analyzing the transition-layer structure it is convenient to consider, instead of intensity, the following variable parameter:

$$\tilde{I}(\Delta\theta) = [I(\theta)\Delta\theta^2/I_0A(\theta)] = \left| \sum_{n=1}^{N} X_n \exp[iQ(n-N-1)](1-e^{iQ})+1 \right|^2. \tag{3}$$

For an ideal crystal the magnitude of $\tilde{I}(\Delta\theta)$ should not depend on $\Delta\theta$. Any deviation of $\tilde{I}(\Delta\theta)$ from unity is indicative of some crystal structure disturbance near the surface and makes it possible to obtain information on the transition-layer structure. One should note, however, that, mathematically speaking, the reconstruction of $N$ parameters $X_n$ for a given function $\tilde{I}(\Delta\theta)$ is an ambiguous problem. Indeed, if some set of parameters $X_n$ represents a solution, then the set

$$\tilde{X}_n = 1 - X_{N-n+1} \tag{4}$$

would also be a solution of the problem. For most problems it seems natural to postulate that the Debye-Waller factor should monotonously grow away from the surface. This requirement limits significantly the number of alternative solutions, but even so the problem does not become a single-solution one. Indeed, there still exist two monotonously growing solutions, interconnected by (4).

A characteristic feature of (3) for parameter $\tilde{I}(\Delta\theta)$, obtained on the assumption of atomic-plane displacement absence, is its symmetry with respect to $\Delta\theta$. In this case the expression for the intensity $I(\theta)$ turns out to be asymmetric due to the asymmetry of the $A(\theta)$ coefficient. At experimentally attainable angles $\Delta\theta \sim 2°$, the asymmetry of coefficient $A(\theta)$ turns out to be of the order of 50%.

The sensitivity of the intensity $I(\theta)$ to the structure of individual atomic planes can be demonstrated with the following simple example. The (111) surface of real diamond-type-lattice crystals comprises a boundary 'double layer' (Fig. 2*a*). Let us imagine, however, some other theoretically feasible ideal-surface structure depicted in Fig. 2(*b*). Fig. 2(*c*) presents the diffraction reflection intensity ratio for these two cases. The intensity ratio is determined by the ratio of the corresponding lattice structure-factor squares and is substantially different from unity for large deviations $\Delta\theta$ from the Bragg angle (Fig. 2*c*).

The $\tilde{I}(\Delta\theta)$ parameter proves to be sensitive to deformations of the ideal crystal structure. The observed symmetry of $\tilde{I}(\Delta\theta)$ suggests a lack of surface relaxation. However, in general, in the presence of non-zero atomic plane displacements, the $\tilde{I}(\Delta\theta)$ function is found to be $\Delta\theta$ asymmetric, the degree of asymmetry substantially depending upon atomic plane displacement. Fig. 3 illustrates the $\tilde{I}(\Delta\theta)$ sensitivity to surface relaxation. The $\tilde{I}(\Delta\theta)$ curves plotted here incorporate the experimentally determined Debye-Waller factors of Si for various values of the first two interplanar-distance deviations $\Delta a_1$ and $\Delta a_2$ from the ideal interplanar spacing $a_0$. In Fig. 3, curves I, II and III represent the cases $\Delta a_1 = \Delta a_2 = 0$, $\Delta a_1/a_0 = \Delta a_2/a_0 = -2{\cdot}5\%$ and $\Delta a_1/a_0 = \Delta a_2/a_0 = -5\%$, respectively. The data presented in Fig. 3

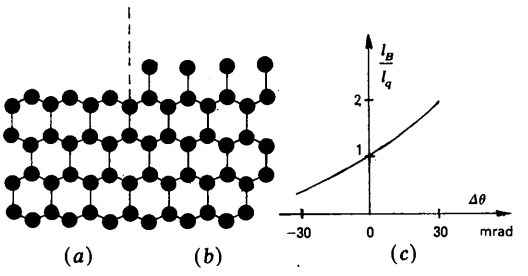


Fig. 2. Influence of crystal-surface structure upon the reflected X-ray intensity in asymptotic Bragg diffraction. (*a*) (111) surface structure of a diamond-like lattice ideal crystal; (*b*) another theoretically possible surface structure for the same crystal; (*c*) computed reflected X-ray intensity ratio in (*a*) and (*b*) as a function of the crystal deviation angle $\Delta\theta$.

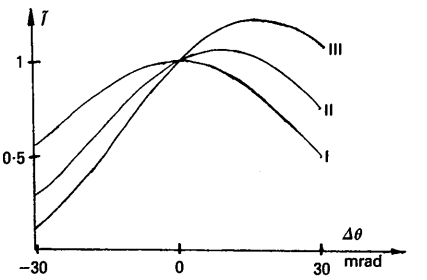


Fig. 3. Influence of surface relaxation on reflected X-ray beam intensity in asymptotic Bragg diffraction conditions. Calculated curves $\tilde{I}(\Delta\theta)$ for different deviations of the first and second interplanar distances $\Delta a_1$ and $\Delta a_2$ ($\Delta a_1/a_0 = \Delta a_2/a_0 = 0$, $-2{\cdot}5$, $-5\%$ for curves I, II, III, respectively).

demonstrate the ability of the asymptotic Bragg diffraction method to detect the displacements of several surface-adjoining atomic planes with an accuracy of the order of 1%. This is sufficient for observing the pure surface relaxation, which according to LEED data (van Hove & Tong, 1979) should be several %.

### 3. Experimental results

Measurements of the diffraction scattering intensity at angles, essentially differing from the Bragg angle, were performed using the triple-crystal X-ray diffractometry (TCD) method, described in more detail by Eisenberger, Alexandropoulos & Platzman (1972), Iida (1979), Iida & Kohra (1979), Afanas'ev, Koval'chuck, Lobanovich, Imamov, Aleksandrov & Melkonyan (1981) and Aleksandrov, Afanas'ev & Melkonyan (1981). The method consists in studying the X-ray flux as a function of analyzer-crystal rotation angle and measuring rocking curves, each usually exhibiting three peaks, namely, the main peak, the pseudo-peak and the diffusion peak.

The main peak is due to the diffraction at the specimen crystal. The pseudo-peak characterizes the reflection curve of the monochromator crystal. The diffuse peak is due to X-ray scattering on the specimen-crystal lattice defects. The TCD method makes it possible to separate these peaks and to study the purely diffractive reflection. Fig. 4 shows some typical TCD rocking curves.

The main peak amplitude depends on the intensity of X-ray beam reflection from the specimen at some angle $\theta$, substantially different from the Bragg angle. The main peak shape is determined by Bragg reflection from the monochromator crystal and should remain invariable over the entire angle range considered. Experimentally, the shape of the main peak was shown to remain practically the same over the whole angular interval ranging up to $6\times10^3$ arc s. This angular interval exceeded the principal main peak half-width by a factor of almost $10^3$. The main peak broadening did not exceed 10% at maximum deviation from the Bragg angle. The constancy of the main peak shape provided unambiguous evidence that the main peak was due to pure-diffraction reflection. The absence of any diffuse peak in Fig. 4(*b*) can be attributed to the presence of comparatively few bulk defects in the specimen.

At small $\Delta\theta$ deviations from the Bragg angle the diffraction intensity is due to the effect of very many atomic planes and is independent of the transition-layer structure. As a result, the $I(\theta)(\Delta\theta)^2$ product should be a constant, which is illustrated by the $I(\theta)\Delta\theta^2/I_0$ experimental data, plotted in Fig. 5 for Si at small values of $\Delta\theta$.

At large specimen deviation angles $\Delta\theta$ the diffraction intensity is substantially dependent upon the transition-layer structure.

Plotted in Fig. 6 is $\tilde{I}(\Delta\theta)$ as a function of the specimen deviation angle $\Delta\theta$ for Ge and Si crystals with superfinish surface treatment (the Ge crystal was deep-polishing etched). The specimens were oriented in the (111) plane. The measurements were carried out using Cu $K\alpha$ radiation.

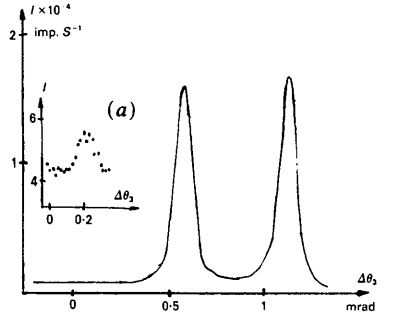


Fig. 4. Intensity of crystal-reflected X-ray beam as a function of the analyzer-crystal rotation angle $\Delta\theta_3$. Ge monocrystal, 111 reflection, Cu $K\alpha$ radiation, specimen-crystal deviation angle $\Delta\theta = -0{\cdot}6$ mrad [in the case of curve (*a*) with only the main peak plotted $\Delta\theta = -30$ mrad].

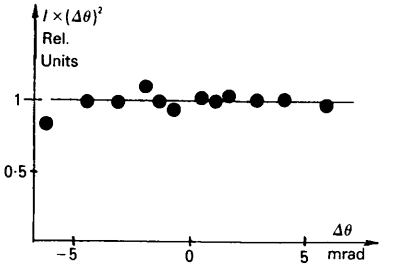


Fig. 5. Dependence of parameter $I(\theta)(\Delta\theta)^2/I_0$ upon crystal deviation angle $\Delta\theta$. Small-angle $\Delta\theta$ data. (Si monocrystal, 111 reflection, Cu $K\alpha$ radiation.)

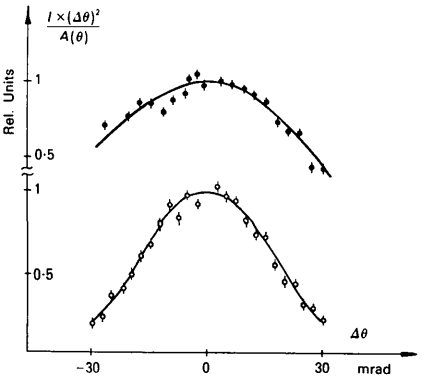


Fig. 6. Dependence of parameter $\tilde{I}(\Delta\theta)$ upon crystal deviation angle in asymptotic Bragg diffraction conditions. Unfilled and filled points indicate the Ge monocrystal and Si monocrystal experimental data, respectively (111 reflection, Cu $K\alpha$ radiation). The theoretical curves were computed according to (3) with optimal parameter choice.

Table 1. *Experimental data analysis*

$n$ = atomic plane number (from the surface); $X_n$ = $n$th-plane Debye–Waller factor; $\tilde{X}_n$ = conjugated $n$th-plane Debye–Waller factor; $\langle u_n^2\rangle^{1/2}$ = root-mean-square atom excursion out of the $n$th plane.

| | Ge | | | | Si | | | |
|---|---|---|---|---|---|---|---|---|
| $n$ | $X_n \pm 0{\cdot}05$ | $\langle u_n^2\rangle^{1/2}$ (Å) | $\tilde{X}_n \pm 0{\cdot}05$ | $\langle \tilde{u}_n^2\rangle^{1/2}$ (Å) | $X_n \pm 0{\cdot}05$ | $\langle u_n^2\rangle^{1/2}$ (Å) | $\tilde{X}_n \pm 0{\cdot}05$ | $\langle \tilde{u}_n^2\rangle^{1/2}$ (Å) |
| 1 | 0·3 | 0·9 | 0·3 | 0·9 | 0·6 | 0·5 | 0 | 0 |
| 2 | 0·4 | 0·7 | 0·3 | 0·9 | 0·6 | 0·5 | 0·1 | 1·1 |
| 3 | 0·7 | 0·4 | 0·6 | 0·5 | 0·9 | 0·3 | 0·4 | 0·7 |
| 4 | 0·7 | 0·4 | 0·7 | 0·4 | 1 | 0 | 0·4 | 0·7 |

Taking into account the present experimental error margins, the observed symmetry of the experimental curves $\tilde{I}(\Delta\theta)$ means that in both Ge and Si crystals the atomic-plane displacements within the crystal–oxide transition layer were less than 1% of the ideal-crystal inter-plane spacings.

Since the angular scale of the observed $\tilde{I}(\Delta\theta)$ departure from unity comprised several thousand arc s, the characteristic thickness of the disturbed layer was about 1–1.5 nm. Consequently, the Debye–Waller factors had to be determined in the discrete model approximation, assuming the disturbance to be localized in the first four atomic layers. We found the Debye–Waller factors by varying the $X_n$ parameters in (3) until reaching the best possible fit of theory to experiment under the requirement of Debye–Waller-factor monotonous growth in the direction away from the surface. Table 1 presents the results of experimental data analysis. One should emphasize that the Debye–Waller factor for the fourth atomic layer in Si turned out to be 1. This means that actually only the first two layers were disturbed (since $X_3 = 0{\cdot}9$ is close to 1). In the variation procedure for establishing the Debye–Waller factors, their weak $\Delta\theta$ dependence was actually taken into account, enabling us to obtain unambiguous expressions. However, with the present experimental error margins the asymptotic Bragg diffraction seems unable to make a choice between the thus found Debye–Waller-factor values $X_n = \exp[-W_n(\theta_B)]$ and the corresponding 'conjugated' values $\tilde{X}_n = 1 - X_{5-n}$. For this reason the 'conjugated' factors are also included in Table 1.

The deviation of Debye–Waller factor from unity can be due not only to atom oscillations and displacements but also to the absence of some of the atoms in the atomic planes near the crystal surface. Assuming the Debye–Waller factors to depend exclusively on atom displacements, one can compute the root-mean-square atom excursion out of the atomic plane for each separate plane. These values also appear in Table 1.

Fig. 7 sketches the schematic structure of the transition layer. Here the regions (*a*), (*b*) and (*c*) represent the ideal crystal, the transition layer under investigation and the invisible-to-X-rays amorphous oxide film, respectively.

The present investigation demonstrates the real possibility of using X-ray diffraction for the study of crystal structure perfection degree and of subsurface atomic plane relaxation at the level of individual crystal planes.

At present, the most wide-spread surface-study technique is indeed the low-energy electron diffraction (LEED) method (van Hove & Tong, 1979). This method provides reliable information on pure surface reconstruction (crystal structure of the surface) and on relaxation of the first sub-surface planes. However, the method requires complicated mathematical processing of the experimental data and special experimental techniques for obtaining super-pure surfaces. Besides, the LEED application is restricted to no more than several surface-adjoining layers, which makes it impossible to investigate transition layers at the boundary of either two crystals or a crystal and an amorphous film.

The asymptotic Bragg diffraction method makes it possible to study not only thin subsurface crystal layers but also the structure of an ideal crystal–amorphous film boundary or the structure of a two-crystal interboundary, the crystals having substantially different interplanar distances. Although the present work was actually concerned with the ideal crystal–oxide-film transition-layer investigation, the asymptotic Bragg diffraction method could also be used for super-pure-surface structure analysis.

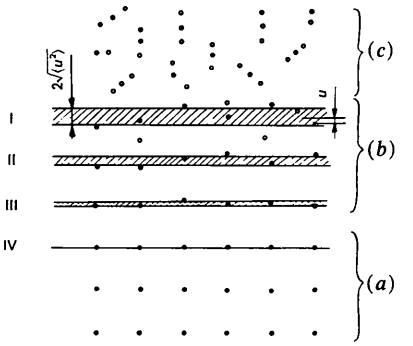


Fig. 7. Schematic structure of the transition layer between a semiconductor and a natural oxide film. Roman figures denote the order number of each reflecting plane. Regions (*a*), (*b*) and (*c*) represent the undisturbed crystal, the transition layer and the amorphous oxide film, respectively.

**References**

AFANAS'EV, A. M., ALEKSANDROV, P. A., IMAMOV, R. M., LOMOV, A. A. & ZAVYALOVA, A. A. (1984). *Acta Cryst.* A**40**, 352-355.

AFANAS'EV, A. M., KOVAL'CHUK, M. V., LOBANOVICH, E. F., IMAMOV, R. M., ALEKSANDROV, P. A. & MELKONYAN, M. K. (1981). *Sov. Phys. Crystallogr.* **26**, 13-20.

ALEKSANDROV, P. A., AFANAS'EV, A. M. & MELKONYAN, M. K. (1981). *Sov. Phys. Crystallogr.* **26**, 725-729.

EISENBERGER, P., ALEXANDROPOULOS, N. G. & PLATZMAN, P. M. (1972). *Phys. Rev. Lett.* **28**, 1519-1525.

HOVE, M. A. VAN & TONG, S. I. (1979). *Surface Crystallography by LEED.* Berlin: Springer.

IIDA, A. (1979). *Phys. Status Solidi A*, **54**, 701-706.

IIDA, A. & KOHRA, K. (1979). *Phys. Status Solidi A*, **51**, 533-542.

YAKIMOV, S. S., CHAPLANOV, V. A., AFANAS'EV, A. M., ALEKSANDROV, P. A., IMAMOV, R. M. & LOMOV, A. A. (1984). *Pis'ma Zh. Eksp. Teor. Fiz.* **39**, 3-5.

*Acta Cryst.* (1986). A**42**, 122-127

# Space and Time Inversion in Physical Crystallography

BY I. S. ZHELUDEV

*Institute of Crystallography, USSR Academy of Sciences, 59 Leninskii Prospect, Moscow* 117333, *USSR*

(*Received* 17 *June* 1985; *accepted* 11 *October* 1985)

## Abstract

Conventional (point) symmetry, antisymmetry, magnetic and complete symmetry are used for the description of specific features of space, time and some crystallographic phenomena. The Onsager principle is extended to phenomena described by second-rank axial tensors. As a result it is seen that the symmetric part of such a tensor changes the sign on time reversal. The actions of two operations - time reversal $R$ and time inversion $T$ ($T=\bar{1}$, 'spatial inversion') - are compared. It is shown that the equations of crystal physics derived by Voigt are in agreement with the Onsager principle.

## Introduction

A formal (analytical) apparatus of tensor crystallography based on the works by Curie, Neumann, Voigt and Shubnikov permits one to predict important symmetry characteristics for different physical phenomena occurring in crystals. The simplest example is the pyroeffect which may, although not necessarily, be revealed in a polar crystal with a special (unique) polar direction. On the other hand, symmetry characteristics allow one to state that if the symmetry conditions are violated the phenomenon under consideration cannot be revealed at all. For example, the pyroeffect (in the generally accepted sense) in centrosymmetric crystals cannot be detected, *i.e.* it is forbidden. The above statements are based on the concepts of conventional point symmetry using orthogonal transformations in three-dimensional space (proper and improper rotations, group $O_3$).

Works on thermodynamics of irreversible processes and, first and foremost, the Onsager (1931) work have established the additional symmetry requirements for some phenomena to be realized. They follow from invariance of relationships describing physical phenomena with respect to time reversal $R$ ($t \rightarrow -t$). Some phenomena (*e.g.* magneto-electric effect) which are allowed from the standpoint of orthogonal spatial transformations cannot be physically realized in all crystals, the relationships describing these phenomena, generally speaking, do not meet the requirements imposed on them by operation $R$ (Landau & Lifshitz, 1979).

Antisymmetry (Shubnikov & Belov, 1964) and magnetic symmetry (Sirotin & Shaskol'skaya, 1982) provide the allowance for requirements imposed by both operations $R$ and the operations inherent in the $O_3$ group. At the same time, practice shows (see below) that the use of magnetic symmetry eliminates some difficulties, giving rise to others. This necessitates the introduction (in addition to symmetry) of physical characteristics of crystals under consideration, *i.e.* a concept concerning two types of crystals - those having a magnetic structure (Landau & Lifshitz, 1960) and those without it. The situation seems to be rather peculiar - to judge some, say, magnetic properties of a crystal, *e.g.* piezomagnetism or magnetoelectric effect, on the basis of magnetic symmetry of the crystal one should know *a priori* whether the crystal is magnetic or not.

Therefore, it is very important to establish purely symmetric characteristics of physical phenomena in crystals which are to be used (after due account of crystallophysical relationships in terms of time reversal $R$) in a way similar to that used at the beginning of this article. In the following this problem is solved within the framework of complete symmetry (Zheludev, 1983).

0108-7673/86/020122-06$01.50 